Journal of Hydrology: Regional Studies 40 (2022) 101045

Contents lists available at ScienceDirect

Journal of Hydrology: Regional Studies

journal homepage: www.elsevier.com/locate/ejrh

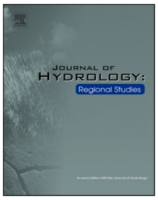

Carbon dissolution effects on pH changes of RAMP lakes in northeastern Alberta, Canada[☆]

F.J. Castrillon-Munoz[a,*], J.J. Gibson[b,c], S.J. Birks[a,b]

[a] InnoTech Alberta, 3608 - 33 St NW, Calgary, Alberta T2L 2A6 Canada
[b] University of Victoria, Geography, Victoria, BC V8W 3R4 Canada
[c] InnoTech Alberta, 3–4476 Markham Street, Victoria, BC V8Z 7X8 Canada

ARTICLE INFO

Keywords:
Lake chemistry
Major ions
Carboxylic acid
PH
Acidification
TDS
Isotopes

ABSTRACT

Study region: This study focuses on boreal lakes in the Athabasca Oil Sands Region (AOSR), Alberta, Canada between latitude 55.68°N and 59.72°N and longitude 110.02°W and 115.46°W.

Study focus

This study focuses on interpretation of hydrochemistry from 50 lakes thought to be acid sensitive, and so monitored by the Regional Aquatic Monitoring Program (RAMP) over the last two decades. This study uses basic statistics, principal component analysis, lithological evidence, CO_2 saturation estimates, mineral equilibria and $\delta^{13}C_{DIC}$ measurements to describe and assess controls on pH and to investigate causal factors of observed pH increase in the lakes.

New hydrological insights for the region: Our assessment provides evidence of two main geochemical processes that control pH increase, namely carbonate dissolution and organic matter uptake, the latter a particularly important component of alkalinity in low pH lakes. Lakes in all subregions show strong evidence of dissolution of marine carbonates of undetermined source, and lake water appears to be trending from CO_2 super-saturation towards atmospheric CO_2 equilibrium. This supports the hypothesis of carbonate input due to permafrost thaw via surface or groundwater pathways, but also reveals likely influence from CO_2 dissolution mechanisms related to climatic influence on ice cover duration.

1. Introduction

Lakes are a key element of the wetland-rich land mosaic in northeastern Alberta, serving to regulate water chemistry, influence the timing of wetland runoff generation to local tributaries and rivers (Gibson et al., 2015), as well as to influence climate at the regional scale through exchange of heat and water with the atmosphere (Krinner, 2003). While lake and ecosystem acidification has been widely observed for industrialized areas of eastern Canada and the United States (Environment Canada, 2005), acidification has only recently become a concern in western Canada, particularly within Alberta and Saskatchewan, due to major developments within the energy sector including bitumen mining, insitu extraction, and upgrading (Hazewinkel et al., 2008; Scott et al., 2010; Jeffries et al., 2010). Acidification takes place when deposition of strong acid precursors, primarily oxides of sulfur (S) and nitrogen (N) in wet and dry forms, exceed the base cation supply to the ecosystem (Scott et al., 2010). For lakes, the base cation supply is typically controlled by

---

[☆] Special Issue on Water and Environmental Management in Oil Sands Regions

[*] Corresponding author.

E-mail address: francisco.castrillon@innotechalberta.ca (F.J. Castrillon-Munoz).

https://doi.org/10.1016/j.ejrh.2022.101045
Received 10 September 2021; Received in revised form 30 January 2022; Accepted 21 February 2022

the chemistry of watershed runoff (Henriksen et al., 1992), but undoubtedly may also be influenced by water-rock interactions and chemical equilibria occurring in soils or within the receiving water body (e.g., Jin et al., 2010). The Regional Aquatics Monitoring Program (RAMP), an industry-funded monitoring program initiated in 1997 and operated by Alberta Environment and Parks, has maintained a lake water chemistry sampling network across the Alberta Oil Sands Region (AOSR) since 1998. Annual lake sampling has been carried out in late summer for 50 lakes, 40 of which are located within 200 km of the center of oil sands operations near Fort McMurray (Fig. 1). The lakes span six representative subregions of northeastern Alberta including the Stony Mountains, West Fort McMurray, Birch Mountains, Muskeg Mountains, Caribou Mountains and Precambrian Shield (Gibson et al., 2010a,b).

While initial assessments based on only a few years of water chemistry data had predicted eventual acidification in many lakes (i.e., pH decreases) due to widespread exceedance of the critical loads of acidity estimates (e.g., Bennett et al., 2008), longer-term sampling over almost 2 decades has since revealed an unexpectedly monotonic increase in the pH in 46 of the 50 lakes (see Gibson, 2019; Gibson et al., 2019a, 2020). Gibson et al. (2016) also identified a subset of RAMP lakes with higher water yields and with tritium levels at intermediate values between 1960s and 2016, attributed to thawing of permafrost and higher runoff, mostly from bog-dominated peat plateaus. A conceptual model proposed by Gibson et al. (2020) postulated that permafrost thaw within the watersheds, which has

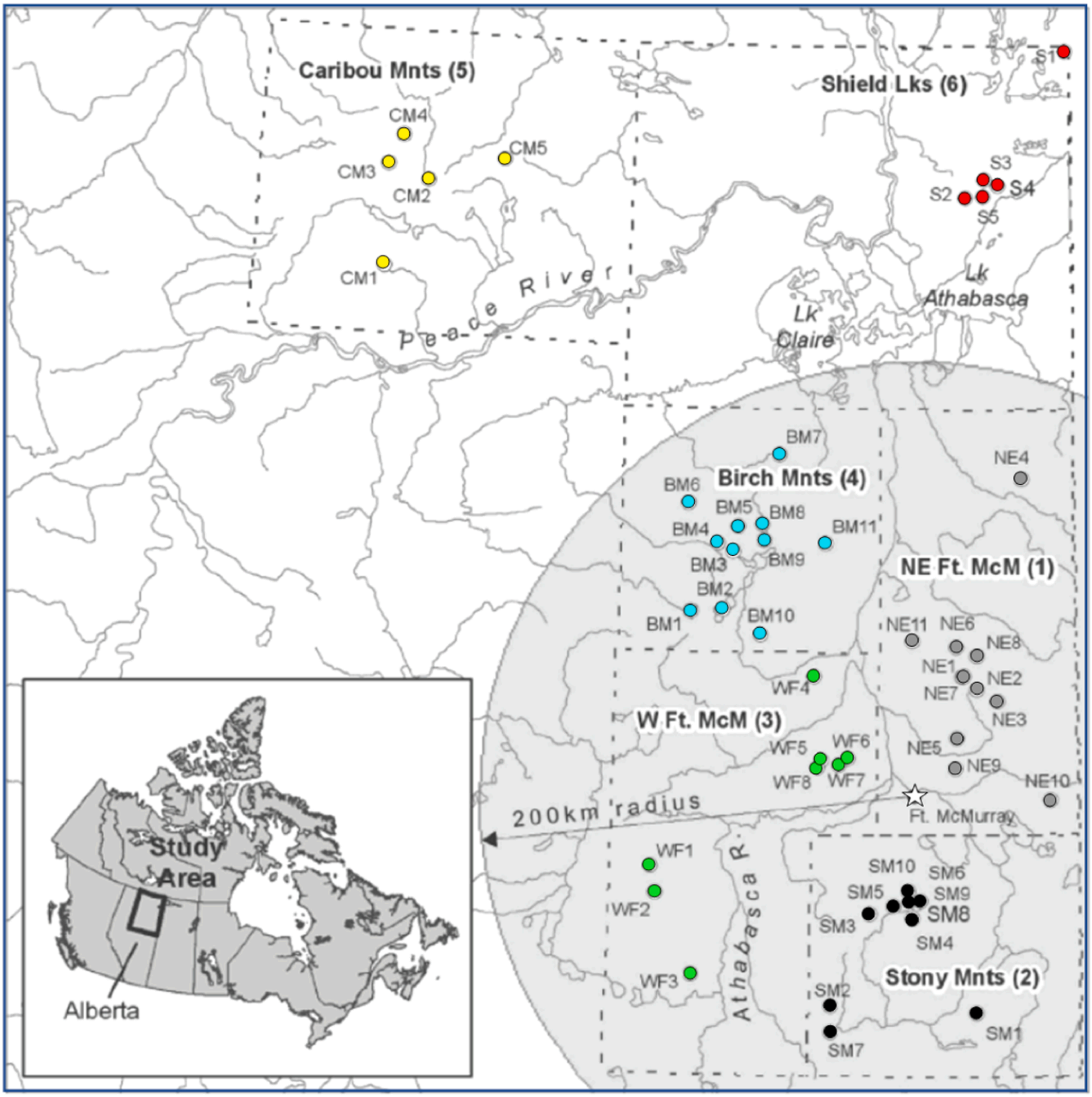

Fig. 1. **:** Map showing lakes in northeastern Alberta color coded by subregion. 40 of 50 lakes are situated within a 200 km radius of the city of Ft. McMurray (after Bennett et al., 2008).

caused bog and fen collapse, may actively be altering runoff processes, contributing to increased mobilization of inorganic carbon, base cations, and other constituents supplying lakes. Essentially, this can be viewed as a reversal, albeit temporary, of the expected long-term acidification trend that was predicted due to regional increases in acidifying emissions. Importantly, Gibson et al. (2020) suggested that runoff increases and associated chemical mobilization are likely to be temporary if they are linked to the permafrost thaw cycle, which has been demonstrated to initially produce increases and then decreases in runoff amounts depending on permafrost extent, as was recently demonstrated for lake-rich regions of Tibet and coastal Northern Canada (Wan et al., 2019, 2020). The temporal effect of other factors such as the CO_2 atmospheric concentration needs further study in the region. Similar changes in chemical transport of dissolved inorganic carbon, base cations and other constituents (i.e., allochthonous sources) has been widely observed for these and other watershed systems undergoing permafrost degradation (e.g., Roberts et al., 2017).

There are many additional investigations that have provided insight into pH regulation and alteration in boreal lakes including study of forest management practices (e.g., Prepas et al., 2001; Gibson et al., 2002b; Devito et al., 2005; Smerdon et al., 2005), surface/groundwater interaction (Schmidt et al., 2010; Birks et al., 2019), and runoff mapping (Gibson et al., 2019a), in addition to the aforementioned acidification research.

Processes influential in controlling pH are briefly reviewed, including autochthonous (within-lake) processes such as dissolved inorganic carbon (DIC) speciation, whereby CO_2 uptake produces a shift to greater proportions of HCO_3^- (Wolfe, 2001), evasion and photosynthetic regulation of respired CO_2 to the atmosphere (Wolfe, 2001), which may be enhanced by increases in ice-free duration (Kling et al., 1992), decomposition (oxidation) of organic matter leading to DIC production (Mattson and Likens, 1992), and organic matter reduction or methanogenesis (reduction) leading to DIC production (Mattson and Likens, 1992; Clayer et al., 2018). Allochthonous (external) processes controlling pH include catchment weathering and leaching of carbonate-rich soils followed by transport of DIC by surface or groundwater discharge to lakes, or due to enhanced DOC loads followed by in-lake mineralization (Hanson et al., 2011). Allochthonous changes may occur due to increases in pH within peatlands flowing into the lakes, a scenario that might be expected to occur in the case of bog or fen collapse due to permafrost thawing (e.g., Gibson, 2019) in presence of an external source of alkalinity.

Anthropogenic greenhouse gas emissions associated with global climate warming are also potentially important controls on carbonate solubility in lakes. CO_2, CH_4 and SO_x and NO_x emissions within the AOSR have been measured or estimated, as reported by Liggio et al., (2016, 2017); and (2019) and the associated impacts on vegetation and aquatic environment have been evaluated by Jung and Chang (2012), Aherne and Posch (2013) and Brook. et al. (2019). An evaluation of areal atmospheric base cation deposition to aquatic ecosystems in Alberta and Saskatchewan from fugitive emissions showed exceedances to critical loads that might represent potential acidifying effects (Makar et al., 2018). However, Makar et al. (2018) also showed that loadings decreased rapidly within the AOSR and that the acid neutralization capacity was likely insufficient to neutralize the S and N deposition within watersheds. From such evaluations, which don't appear to account for the observed pH increases, we suggest that base cation buffering may not be the only important pH regulation mechanism for RAMP lakes. Cook et al., (2017) hypothesized that the base cation budget is dominated by groundwater and watershed inputs and that carbonate dissolution exerts a first order control over lake sediment geochemical composition mainly though groundwater influence. Groundwater recharge, surface water/groundwater interaction and permafrost thaw are expected to leave geochemical and isotopic fingerprints on lake water similar to that noted for area rivers (Jasechko et al., 2012; Gibson et al., 2013; Birks et al., 2018, 2019) and may play a direct or indirect role in controlling the pH of runoff and/or lake water. While major ion signatures are explored here in some detail for the RAMP lakes, an expanded array of solute isotopic tracers that may provide additional insight into the role of groundwater in the lake budgets remains a potential avenue to explore in future investigations.

From a study of hardwater boreal lakes, Finlay et al. (2015) suggested that spring and summer pH increases were likely attributable to climate warming process that reduce ice cover or increase the permafrost thaw, thus reducing the amount of CO_2 stored under ice and increasing the chemical uptake of CO_2.

In a similar way, we sought to test the relative importance of the many proposed geochemical mechanisms. Our initial hypothesis was that carbonate dissolution within the lakes and possibly within the entire watershed areas, enhanced groundwater and surface water inputs of water with high mineral content, and CO_2 dissolution triggered by permafrost thaw and influenced by reduced lake ice cover, were the most influential processes, whereas factors such as S and N emissions were considered to be secondary (Lajewski et al., 2003).

This paper provides a comprehensive analysis of major ion water chemistry measurements made during 1999–2015 for the 50 RAMP lakes including graphs, basic statistics and principal components analysis (PCA) to support the discussion of important geochemical mechanisms and patterns among the various subgroups. We also utilize mineral and CO_2 solubility calculations based on the geochemical program PHREEQC to evaluate and discuss evidence of the relative importance of various lake pH regulation mechanisms, and importantly, to constrain possible causes of the observed region-wide pH increases. Finally, we endeavor to identify implications of such processes for regional sustainability of lakes, and address challenges for monitoring oil sands development impacts in a landscape experiencing pronounced and ongoing climatic changes.

2. Methods

2.1. Site locations

The RAMP lakes, situated in the boreal region of Alberta, are comprised of several regional upland plateaus and lowland plains subregions. The lakes situated within 200-km radius of Fort McMurray include ten lakes in the Stony Mountains (SM), eleven lakes in the Birch Mountains (BM), eight lakes west of the city of Fort McMurray (WF) and eleven lakes in the northeast (NE) Muskeg Mountains (Fig. 1). Lakes situated outside of the 200-km radius include five Precambrian Shield lakes to the west of Lake Athabasca (S) and five lakes in the Caribou Mountains (CM). The lakes range from small (3.4 ha) to large (4400 ha), with depths ranging from 1 to 30 m. Watersheds vary in size from 57 ha to 16,555 ha, with percentage lake area ranging from 1% to 30% (Gibson et al., 2015, 2019a, 2020). We note that the smallest and largest lakes in the RAMP network are both less than 10% of the area of the smallest and largest lakes studied by Finlay et al. (2015), which is relevant for the discussion later on.

The RAMP lakes are situated predominantly in headwater catchments across a range of latitude, morphometry and wetland-rich landscapes (Gibson et al., 2010a,b). The headwater locations were preferentially selected to evaluate atmospheric deposition associated with acidifying and neutralizing emissions and particulates. The lakes in the Stony and Birch Mountains are situated on peat plateaus underlain by weathered shales of the Cretaceous Colorado Group that form a shallow, low-permeability barrier to vertical groundwater movement. Shield lakes are situated in areas underlain by crystalline Precambrian Shield bedrock covered by a shallow, discontinuous mantle of glacial till. In all other subregions (NE, SM, WF, BM, CM; Fig. 1) subregions, lakes are underlain by Quaternary tills, sandstones, siltstones, shales and carbonates of Cretaceous to Devonian age. The lowland lakes typically have higher permeability than the peat plateaus which likely implies greater potential for groundwater interaction. Buried Quaternary/Tertiary channels are a common feature of the AOSR and, as with stream channels, are locally influential as sources and/or sinks of water for some area lakes (Gibson et al., 2019b).

Evaporation in Alberta lakes has also been investigated as part of water budget studies by Gibson et al. (2002a), (2019a), (2020). Annual evaporation losses from lakes range from site-to-site and year-to-year between 18% and 50% of annual inflow, with minimum values between 4% and 36% and maximum values between 26% and 66%. Lakes with low evaporation/inflow tend to remain relatively low despite interannual variability, whereas lakes with high evaporation/inflow tend to remain high, although they tend to show somewhat higher interannual variability. The lakes west of Fort McMurray (WF) subregion were estimated to have the highest evaporation losses (Gibson et al., 2019a, 2020). One consideration we explore later on is that high evaporation rates may potentially contribute to increasing trends in chemical solutes trends, alkalinity, carbonate mineral saturation, and increased lake pH values.

2.2. *Water sampling*

Due to the high dilution and high sensitivity to strong acids and acid precursors such as organic matter (Cook et al., 2017), it is expected that the RAMP lakes receive a significant percentage of their input from surface water, snowmelt precipitation, from rainfall and dust deposition. Based on previous assessments using radon-222, the groundwater contribution to the lakes is estimated to range from about 1–20% of annual inputs (see Schmidt et al., 2010), although it has not been measured in all RAMP lakes.

Lake water chemistry was sampled annually for electrical conductivity (EC), pH, total dissolved solids (TDS), dissolved inorganic carbon (DIC), dissolved organic carbon (DOC), major, minor, trace ions, stable isotopes (^{18}O and ^{2}H). Stable water isotope results have been described in Gibson et al. (2019a, 2020). Tritium was also collected on a few occasions, as described in Gibson et al. (2016), and $^{13}C_{DIC}$ was collected on one occasion in 2011, as described here for the first time. All samples were water column samples from the euphotic zone collected by float plane or helicopter from the lake center. Collection dates ranged across the months of July, August, September and October from 1999 to 2015, with 89% of samples collected between August and September, clearly after dilution from snowpack melt had already occurred. The sampling methods and lab procedures have been described in Cook et al. (2017), Birks et al., (2018, 2019) and Gibson et al. (2020), and are consistent with approaches used previously in the region.

2.3. *Aqueous ion balance error and ions compensation*

Ion balance errors (IBE) were evaluated to identify acceptance criterion. The IBE estimates are unbalanced in favor of the cations in the majority of water samples, which is frequent in very low salinity waters (TDS range from 5.3 mg.L^{-1} to 128 mg.L^{-1} and mean of 31.1 mg.L^{-1}). In order to improve the IBE results, total and ionized carboxylic acids concentration estimates, C_T and A^-, respectively were applied to the ion balances (Oliver et al., 1983; Whitfield et al., 2010). To estimate A^- the following relationship was applied:

$$[A^-] = \frac{\overline{K}[C_T]}{\overline{K} + [H^+]} \tag{1}$$

where $\overline{K}$; C_T and H^+ are the mass action quotient of the fulvic and humic acids, organic (fulvic and humic) acids concentration and hydrogen ions, respectively.

For the C_T estimate DOC concentration in mg.L^{-1} was factored by 10 μeq. mg^{-1} to each sample. These estimates allowed us to achieve a charge balance of ± 25% as an acceptance criterion (Oliver et al., 1983; Whitfield et al., 2010). After adding A^- to the sum of anions, the majority of samples (80% of the 778 samples) passed this criterion which confirmed that the imbalance was mainly due to the ionized component of the dissolved organic matter (DOM) concentration in the lakes.

2.4. *Speciation and statistical software*

Saturation indices were determined using the equilibrium/mass-transfer model PHREEQC 3.5.0 (Parkhurst and Appelo, 1999). Spearman correlation analysis and principal components analysis were conducted with SigmaPlot for Windows14.0.

3. Results and discussion

3.1. pH trends

In general, pH (-log [H^+]) is found to increase with alkalinity in a sigmoidal shape, flattening at about pH = 8.0 once alkalinity concentrations reached about 800 μeq.L^{-1} (Fig. 2(a), Table 1). Alkalinity and the ions that contribute to the alkalinity, as represented in the equation below:

$$\text{Alkalinity} = [HCO_3^-] + [CO_3^{2-}] + [OH^-] - [H^+] = ([Na^+] + [K^+] + [Mg^{2+}] + [Ca^{2+}] + [NH_4^+] + [Mn^{2+}] + [Fe^{2+}]) - ([Cl^-] + [SO_4^{2-}] + [NO_3^-] + [\text{Organic } A^-]) \quad (2)$$

are increasing temporally directly with organic A^-, and dissolved calcium, as illustrated in Fig. 2(a), Fig. 3 and Table 1. Time-series pH data for lakes, color-coded by subregion, are illustrated in Fig. 2(b), and overall depict increasing pH in all subregions and most individual lakes.

While field atmospheric and in situ lake CO_2 measurements were not a component of this investigation, apparent pCO_2 and field pH values were compared to pH produced in the speciation model at atmospheric pCO_2 equilibrium. Most lakes show an apparent disequilibrium effect between atmospheric pCO_2 and the measured pH, similar.

Temporally, we note continuous slight increments in dissolved chemistry and pH which are evident across the region during the 15 years of sampling (Fig. 2(b)).

to that which has been noted for dilute lakes (Bisogni and Arroyo, 1991), and which is frequently associated with seasonally ice-covered lakes (Wolfe, 2001). The results indicate that most lakes are supersaturated in pCO_2 relative to the atmosphere and the observed field pH is up to one unit lower than the pH at atmospheric equilibrium, suggesting that the RAMP lakes are active sources of CO_2. While based primarily on geochemical modeling, and on a single euphotic zone sample for each lake in late summer, this appears to be consistent from year to year and across the entire lake network, suggesting that CO_2 evasion is likely a systematic ongoing process.

Respiration of CO_2 and accumulation under lake ice between November and April, would contribute to a reduction in pH and the dissolution of carbonates and subsequent release to the atmosphere in spring/summer. Combined with higher temperatures, and CO_2 uptake by phytoplankton and periphyton and/or removal of CO_2 by photosynthesis (Lajewski et al., 2003), this may promote carbonate precipitation and pH lake increase as observed in previous studies (Cole and Caraco, 1998; Finlay et al., 2015). For example, pCO_2 values under ice were found to exceed open water values by 3–14 times for Alaskan lakes (Kling et al., 1992; Wolfe, 2001). High CO_2 evasion takes place during the lake turnover period that possibly goes unrecorded if sampling is conducted in the summer season.

Overall, without seasonal observations or under-ice measurements it is difficult to conclude whether the CO_2 evasion process is close to steady-state interannually or whether there are long-term climate-driven changes in ice cover that have exerted an overall upward influence on pH tendency. While unconfirmed, climate-driven changes in ice cover appear to be at least part of the explanation of the observed pH effect. A more detailed field-based investigation including winter sampling under ice would be particularly informative to test this assertion, and so is identified as a potentially important target for future investigations.

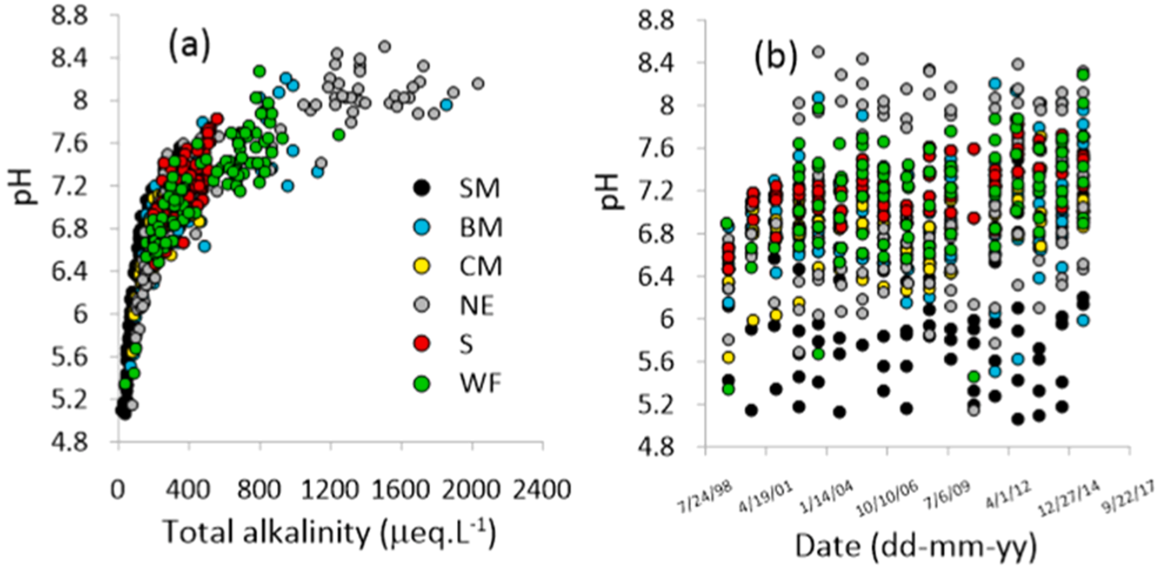

Fig. 2. (a) Total Alkalinity (left) and time (right), (b) as a function of pH for the RAMP Lakes.

Table 1

Summary of statistics for physical and chemical properties of the RAMP Lakes (NE Alberta).

	BM (137)		CM (70)		NE (128)		S (74)		SM (105)		WF (94)	
	Mean	St. dev	Mean	St. dev	Mean	St. dev	Mean	St. dev	Mean	St. dev	Mean	St. dev
Chlor_a (μg/L)	31.71	35.20	10.47	4.06	20.31	16.63	7.90	9.99	10.82	5.36	36.20	51.49
Color (mg/L Pt)	156.03	119.33	210.88	71.06	153.73	98.09	66.38	42.43	84.04	42.15	158.10	123.36
Turb (NTU)	7.30	6.27	2.18	0.75	3.39	1.75	2.18	2.12	2.92	1.43	5.08	7.71
TDS (mg/L)	32.61	15.66	22.56	8.85	41.38	33.16	30.92	6.71	11.88	6.08	39.56	18.83
DOC (mg/L)	21.33	10.93	20.37	3.79	24.73	6.37	16.33	5.05	17.41	4.03	34.43	9.86
TSS (mg/L)	8.05	8.92	2.75	2.11	5.30	5.93	4.16	6.57	2.95	2.61	16.29	34.05
DIC mg/L	3.13	2.40	2.37	1.35	6.11	6.35	4.12	1.17	0.97	0.91	4.62	2.60
pH	6.85	0.52	6.83	0.30	7.07	0.77	7.24	0.19	6.09	0.68	7.03	0.69
Temp (^{o}C)	3.46	1.54	4.91	0.77	2.94	1.67	3.86	1.02	3.00	1.78	2.65	1.42
Ca (μeq.L^{-1})	285.74	147.06	283.03	117.84	446.55	338.65	290.41	82.64	94.45	70.18	433.89	208.07
Mg (μeq.L^{-1})	159.17	84.40	118.13	41.75	233.64	182.73	158.74	34.97	64.00	42.11	235.88	141.62
Cl (μeq.L^{-1})	37.97	58.48	4.99	2.33	5.81	2.98	40.60	16.90	5.21	3.28	9.25	5.95
SO$_4$ (μeq.L^{-1})	121.08	89.39	44.92	18.65	20.22	17.27	19.35	6.91	18.59	9.89	55.50	82.76
K (μeq.L^{-1})	17.65	7.39	7.49	4.16	7.87	5.80	18.70	4.71	14.34	12.08	19.53	7.47
Na (μeq.L^{-1})	129.04	94.70	35.24	13.12	120.12	116.66	91.03	23.35	39.91	13.52	96.76	90.86
TotAlkCarb (ueq.L^{-1})	480.67	325.52	419.15	157.58	785.02	604.92	535.40	71.49	199.08	161.07	751.61	358.01
A (μeq.L^{-1})	164.37	110.00	162.33	38.07	193.17	71.57	147.95	40.64	86.99	68.48	278.92	126.92
pK (μeq.L^{-1})	5.28	0.20	5.28	0.11	5.35	0.27	5.43	0.06	4.98	0.29	5.34	0.26
H+ (μeq.L^{-1})	0.36	0.65	0.24	0.22	0.38	0.61	0.07	0.03	2.14	2.52	0.47	0.98
Ct (μeq.L^{-1})	213.31	109.33	203.70	37.89	247.35	63.72	163.30	50.49	174.13	40.30	344.33	98.60
si_Calcite	-2.94	0.97	-2.92	0.63	-2.44	1.50	-2.31	0.45	-4.68	1.35	-2.48	1.42
pCO2(g) (μatm)	1651.55	0.26	-2.78	0.12	-2.82	0.37	-2.98	0.09	-2.44	0.41	-2.77	0.38
si_Aragonite	-3.10	0.97	-3.08	0.63	-2.61	1.50	-2.47	0.45	-4.84	1.35	-2.64	1.42
si_Dolomite	-6.09	1.94	-6.16	1.26	-5.09	2.97	-4.80	0.79	-9.38	2.51	-5.13	2.67
K/(K+H)	0.78	0.20	0.80	0.12	0.79	0.20	0.91	0.03	0.47	0.30	0.81	0.26
HCO$_3$ +A (ueq.L^{-1})	481.03	325.24	419.39	157.43	785.41	604.58	535.47	71.47	201.23	159.34	752.08	357.27
Na+K (ueq.L^{-1})	146.68	98.20	42.73	16.59	128.00	121.34	109.73	22.50	54.25	20.65	116.29	95.81
A/HCO$_3$	0.63	0.25	0.72	0.22	0.62	0.36	0.43	0.24	0.73	0.25	0.71	0.28
HCO$_3$ (ueq.L^{-1})	316.67	228.67	257.05	128.04	592.23	566.65	387.52	100.53	114.23	94.63	473.17	264.71
SC_Field (μS/cm)	50.95	24.47	35.25	13.83	64.66	51.82	48.32	10.48	18.56	9.50	61.81	29.42
Al_F (ug.L^{-1})	170.31	203.38	61.63	33.28	37.53	49.15	16.68	15.54	70.74	63.09	15.89	12.55
AlkNonC (ueq.L^{-1})	432.54	300.96	393.98	157.08	782.16	599.64	498.94	74.41	188.90	129.10	721.31	359.48

Notes: Chlor a: Chlorophyll_a; Turb: Turbidity; TDS: Total Dissolved Solids; DOC: Dissolved Organic Carbon; TSS: Total Suspended Solids; TCA: Total carbonated alkalinity; A: Ionized carboxylic acids, $[A^{-}] = \overline{K}[Ct]/(K+[H^{+}])$; $p\overline{K}= 0.96 + 0.90\ pH-0.0039(pH)^{2}$; Ct= Total carboxylic acids (Oliver et al., 1983). The number of samples for each sub-region are included in brackets.

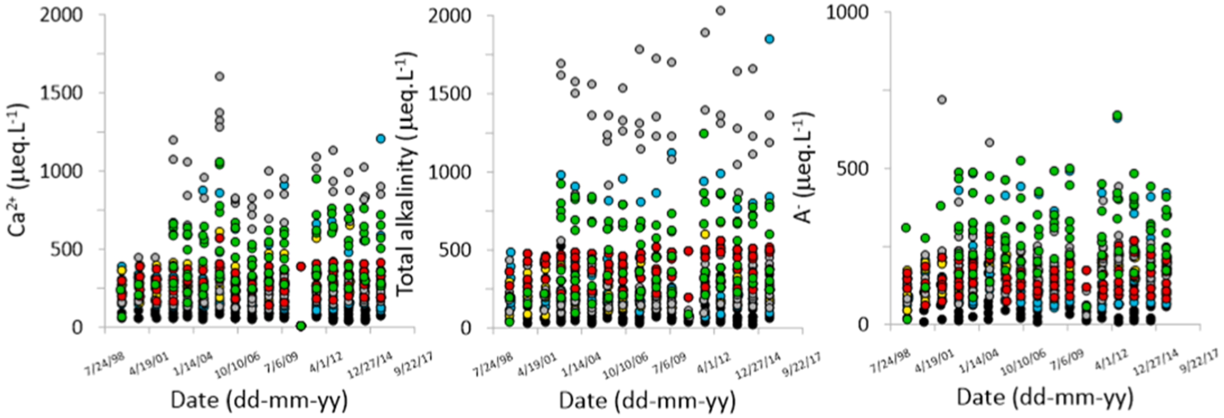

Fig. 3. Calcium, total alkalinity and A- (μeq. L-1) as a function of time for the RAMP Lakes.

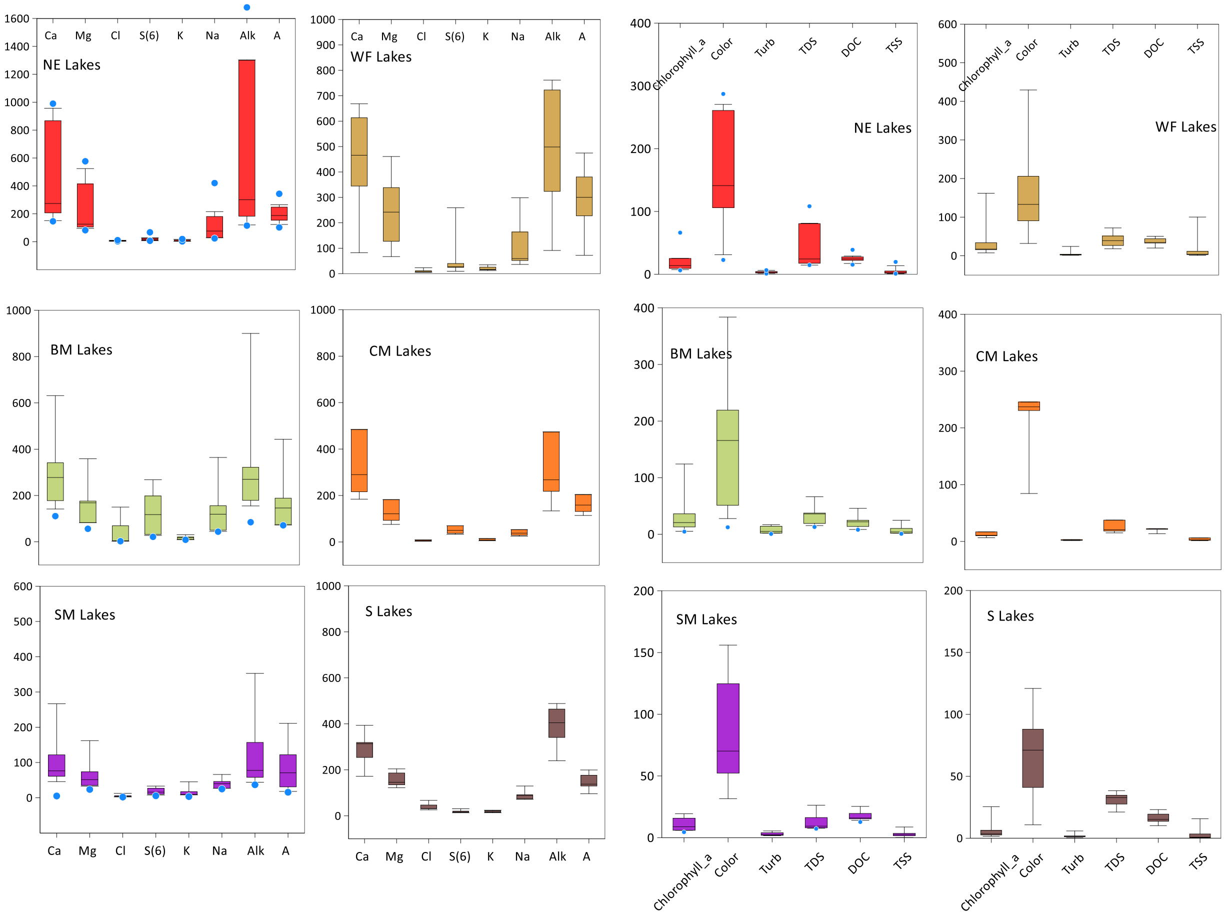

Fig. 4. RAMP Lakes Major ion concentrations (μeq.L^{-1}) and physico-chemical characteristics (mg.L^{-1}). Note: Chlorophyll_a in μg/L and turbidity in NTU. Lakes groups are SM -Stony Mountains, WF-West Fort McMurray, NE-Northeast Fort McMurray, BM-Birch Mountains, CM-Caribou Mountains, S – Shield. Number of sites per group of lakes is as follows: SM (n = 10), WF (n = 8), NE (n = 8), BM (n = 10), CM (n = 5),S (n = 5). The lower box boundary is 25th percentile, the line in the box is the median and the top box line is the 75th percentile. The error bars below and above represent the 10th and 90th percentile with outliers in blue circles; S(6) = SO_4^{-2}.

3.2. Lake water chemistry composition

Based on major ion compositions, the RAMP lakes were classified as Ca-Mg-HCO$_3$-A$^-$ and Ca-Mg-Na-HCO$_3$-A$^-$ water types (Fig. 4, Table 1). The ionized carboxylic acid contribution (A$^-$), from humic and fulvic substances, to the overall ionic balance appears to be of importance for all lakes with the highest mean values of 278 and 193 μeq.L^{-1} for the WF and NE lakes, respectively, near to the oil sands development areas and decreasing in importance with the distance from the oil sands projects towards the BM CM, S and SM lakes with mean concentrations of 164, 162, 147 and 86 μeq.L^{-1}, respectively. In addition, minor concentrations of dissolved SO$_4$ and dissolved Na were found to be present predominantly in the WF, BM and NE lakes. Examination of the physico-chemical characteristics of the lakes reveals that lake water color is an important indicator across the six subregions. The CM lakes showed the highest mean.

color value of the six subregions with 210 mg.L^{-1} Pt (Fig. 3). High water color is also typically associated with low turbidity, with lowest values also observed for the CM lakes at 2.18 mg.L^{-1} The contrast between these two parameters is indicative of watersheds dominated by ombrotrophic peatlands (bogs) and extensive permafrost, which account for 65–88% of watershed land cover for the CM lakes (Gibson et al., 2015, 2020). The high natural color water is reflective of acidity generated by organic matter dissolution (Oliver et al., 1983). Lakes most susceptible to acidification show low alkalinity, low chlorophyll and low color (Eilers et al., 1983).

Principal component analysis (PCA), a multivariate statistical technique, was applied to evaluate the relationships between pH and physico-chemical constituents. PCA biplots for each sub-region (Fig. 5) illustrate loadings for variables (vectors) as well as scores for individual lakes (points). Proximity in the biplots is an indicator of similarity between lakes as well as an indicator of the importance of driving variables. The first principal axis, PC1, was found to account for between 38% and 49% of variability in the sub-region datasets, driven mainly by positive shifts in pH, DIC, alkalinity, and base cations (Ca and Mg), whereas the second principal axis, PC2, found to account for between 13% and 20% of variability in the sub-region datasets, was driven by variables positively correlated with residence time such as color, turbidity, TSS, carboxylic acid and some nutrients. The alignment of variables such as DIC, alkalinity and base cations with pH strongly suggests that carbonate dissolution may accompany pH increases in the lakes. We note slightly different orientation of loadings vectors for shield lakes (S), attributed to fundamentally different weathering mechanisms in this sub-region, although the overall alignment of pH with carbonate dissolution indicators remains similar to other sub-regions within the boreal plains. For WF, BM and CM sub-regions, chloride (Cl$^-$) follows variations driven mainly by PC2 such as color, turbidity, total carboxylic

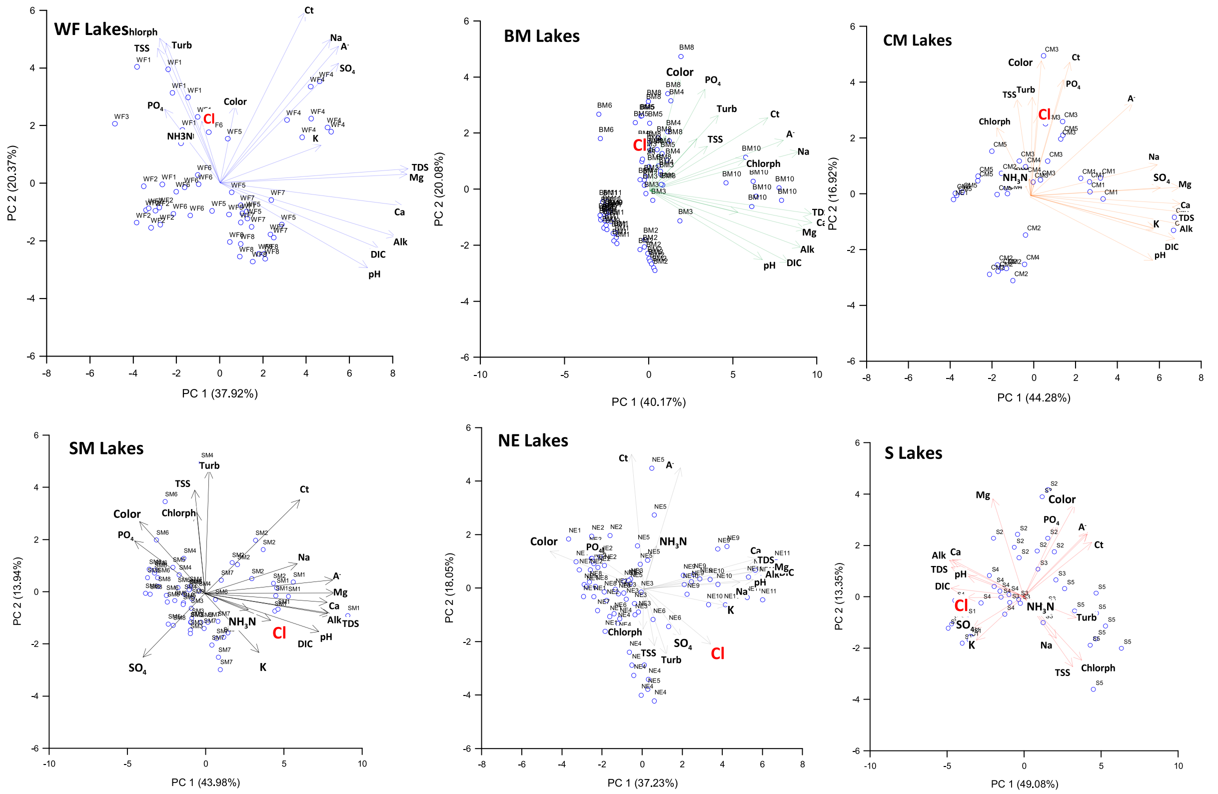

Fig. 5. PCA biplot of RAMP lakes subregions. Each lake number is represented within the symbol. Increments of pH, DIC, alkalinity, base cations (Ca, Mg and K) and TDS are observed along the PC1 in WF, SM, BM, CM and NE. PC2 shows variations of chlorophyl, color, TSS, turbidity PO$_4$ and Ct on the same lake subregions. The S lakes in the Canadian Shield show a opposite direction distribution of the variables mentioned before along the PC1 and PC2. To note the variability of the ion chloride assumed to behave conservatively.

acid (Ct), whereas for NE, SM, and S, Cl^- aligns closely with pH and the carbonate dissolution drivers along PC1. Generally, Cl^- is assumed to behave conservatively along hydrologic flowpaths, although halite dissolution, both active and glaciogenic, are known to be significant sources of Cl^- via springs and seeps emerging along the lower Athabasca River, its tributaries, and to some extent lakes and wetlands (e.g., Saline Lake, Saline Fen). Given that Colorado Shale is present throughout the western subregions WF, BM and CM, we suggest that halite influences would be reduced in these areas compared to sources related to weathering of till or shale. For NE, SM and S sub-regions, where the Colorado Group is absent, we suggest that Cl^- related to such halite dissolution sources may be more important and is possibly may be linked to or concurrent with carbonate dissolution or carbonate weathering. As lakes in sub-region S are situated within crystalline bedrock terrain, the likelihood is that carbonate and Cl- sources are also tracing near-surface inputs to the lakes. The carbonate dissolution hypothesis (Cook et al., 2017) is further discussed and evaluated later on using results from saturation index calculations and stable isotope results.

3.3. *Residence time and TDS*

Gibson et al. (2020) reported residence time estimates for each lake in the RAMP dataset using bathymetry and isotope-based inflows (2002–2017). Ordered from lowest to highest, mean residence times by sub-region were found to be: NE: 0.84 ± 0.46 years; WF: 1.06 ± 0.35 years; SM: 1.14 ± 0.53 years; BM: 2.06 ± 3.32; CM: 2.41 ± 1.02; and S: 3.02 ± 2.75. Residence times for the entire dataset were found to be positively correlated with pH (r^2=0.335, $p = 0.0177$), $\delta^{13}C_{DIC}$ ($r^2 = 0.392$, $p = 0.005$), and Cl^- ($r^2 = 0.291$, $p = 0.0406$), and negatively correlated with color ($r = -0.62$, $p < 0.001$), aluminum ($r^2 = -0.535$, $p < 0.001$), DOC ($r^2 = -0.468$, $p < 0.001$), turbidity ($r^2 = -0.4$, $p = 0.004$), chlorophyll-a ($r^2 = -0.344$, $p = 0.0148$), and most nutrients. Residence time was found to be poorly correlated with TDS and most major ions except as noted.

The NE and WF lakes were found to contain the highest mean TDS concentrations of 41.38 $mg.L^{-1}$ and 39.56 $mg.L^{-1}$, respectively, and the highest mean total carbonate alkalinity (TCA) values of 785 and 751 $\mu eq.L^{-1}$, respectively, and showed a wider spread in pH values, ranging from 5.99 to 8.12 for NE and 5.56–8.3 for WF. The SM lakes were found to have the lowest mean pH value of 6.09, the lowest mean TDS value of 11.8 $mg.L^{-1}$ and lowest mean TCA value of 199 $mg.L^{-1}$ (Table 1).

Overall, widely varying lake residence times produce a broad distribution of geochemical responses including, in some cases, significant differences in ionic dominances, as noted by Shapley et al. (2005). Further work needs to be conducted on the lakes to identify the influence of the residence time on the controls aligned mainly with PC2 (see Fig. 5), although these are not thought to be the primary drivers of pH increases observed in the lakes.

3.4. *CO2, alkalinity and pH*

In Sweden, long term changes in pH related to land use changes including forest fires have been studied and were attributed mainly to release of base cations and alkalinity previously trapped in the watershed soils (Remberg et al., 1993; Korsman and Segerstrom, 1998). Such processes were also postulated to occur in a similar way for systems undergoing significant impacts from climate change. Lajewski et al. (2003) reported historical nitric-acid triggered carbonate weathering in the Finger Lakes, New York at times of high

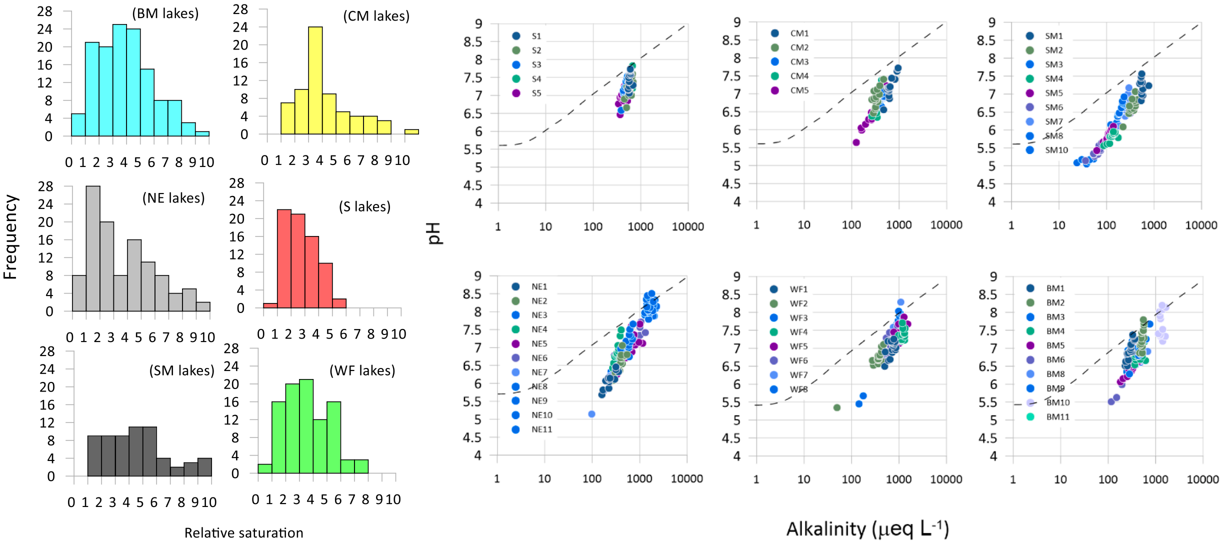

Fig. 6. CO_2 relative saturation of lakes with respect to atmospheric concentration (left) and pH alkalinity and apparent dissolved CO_2 in RAMP lakes (right). The dashed line represents the theoretical equilibrium with the atmosphere at 20 °C (after Cole and Prairie, 2009). Most lakes are supersaturated (below the line however all lakes subregions seem to be trending towards atmospheric equilibrium suggesting that the atmospheric and dissolved CO_2 are buffered by the acid neutralization capacity of the alkalinity. To note several lakes in the NE, WF and BM subregions fall above the theoretical equilibrium line whereas lakes from the CM subregion fall clearly below the line.

summer surface water temperatures. They concluded that efficient photosynthetic removal of CO_2 in surface water led to supersaturation with respect to calcite and resulted in increased alkalinity and pH values during summer. Houle et al. (2010) in a study of lake chemistry of 47 temperate and boreal catchments in North America and Europe between 1989 and 2005, found that climate-related annual temperature increases were more strongly correlated with pH and alkalinity of the lake than with reduction in S deposition, which were decreasing steadily in most areas due to emissions reductions.

The role of S and N from fugitive dust emissions on pH control via dissolution of carbonates was considered as a secondary process to increased summer surface water temperature, picoplankton concentrations and/or removal of CO_2 by photosynthesis (Lajewski et al., 2003) and other processes such as CO_2 degassing and carbonate dissolution in lakes. It is possible that S and N acidifying emissions dissolved in the rainfall and snowmelt play a role in carbonate dissolution within aquifers in recharge zones, however, these would be secondary to the main role that the dissolved CO_2 in the rainfall might play. Additional efforts are required to understand the role of the dust and the acidification precursors on carbonate dissolution in the recharge zones of AOSR in Alberta.

Table 1 provides a statistical summary of the general chemistry which includes apparent pCO_2 and measurements of DIC. These parameters are in agreement with the pH data which allows us to infer that most of DIC exists in the form of bicarbonate rather than as CO_2 within the lakes. However, a preliminary comparison of apparent dissolved CO_2 concentration (ppm) in the lakes relative to the measured dry atmospheric concentration (mean = 394 ppm) for the AOSR (Liggio et al., 2019) provides first evidence that most lakes are CO_2 supersaturated, with most lakes showing supersaturations up to six times that of atmospheric CO_2 (Fig. 6 left). These results indicate that most lakes fall below the theoretical equilibrium line therefore constitute a net source of CO_2 to the atmosphere (Cole and Prairie, 2009) during the open-water period from May/June to October (Fig. 6 right). However, all lakes subregions seem to be trending towards atmospheric equilibrium suggesting that the atmospheric and dissolved CO_2 are buffered by the acid neutralization capacity of the alkalinity. Several lakes in the NE, WF and BM subregions fall above the theoretical equilibrium line whereas lakes from the CM subregion fall clearly below the line. Lakes that fall above the theoretical equilibrium line are hardwater lakes with pH above 8.0.

CO_2 sources to the lake are expected to include photosynthesis, plant respiration in deep lakes, and terrestrial watershed inputs. In lakes with short hydrologic residence times, groundwater is sometimes the cause of high dissolved CO_2 concentrations (Cole and Prairie, 2009). Other processes that might generate abundant CO_2, such as permafrost thaw (Gibson et al., 2019), also need to be considered. Precipitation-driven run-off augmented by permafrost thaw sources (Gibson et al., 2019) might be one of the key mechanisms to explain the high CO_2 relative saturation in some lakes. However, high dissolved CO_2 content would lead to lake acidification and the trends observed point towards a general acid neutralization effect in all lakes of the region. Thus, understanding the processes triggering the generation of alkalinity is very important to explain the increasing pH trends.

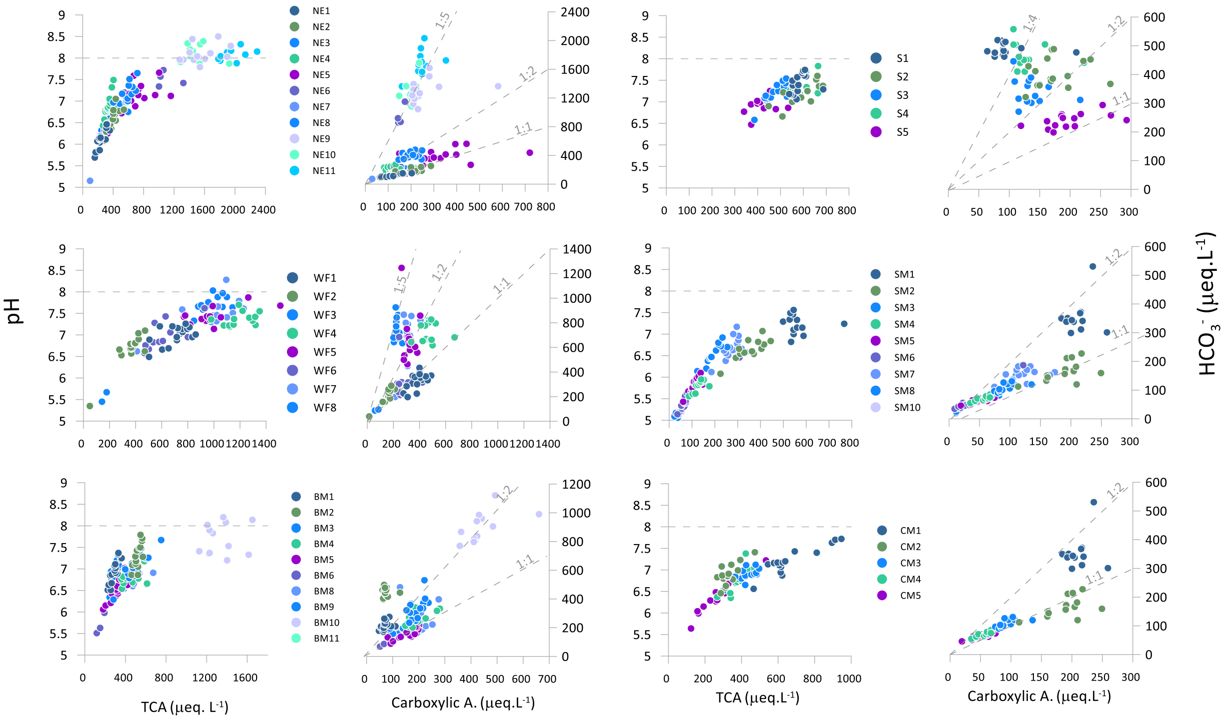

Fig. 7. Relative HCO_3^- and ionized carboxylic acid (A^-) contribution to the total carbonate alkalinity (TCA) in the RAMP lakes. To note the higher contribution from HCO_3^- to some lakes in the NE, WF subregions closer to oil sands operations and the lower contribution at the SM and CM lakes further away from the oil sands operations.

3.5. Ionized carboxylic acid (A-), bicarbonates and pH

The larger contribution of DOC relative to the DIC indicates that dissolved organic matter, present in the form of weak organic acids, are also an important component of the alkalinity and the ion balance (Herzeg and Hesslein, 1984), and contribute to the total alkalinity, thereby buffering the lakes at low values of pH (Fig. 7).

While most lakes fall below the softwater – hardwater lower boundary defined by pH = 8.0 (Fig. 7) (Finlay et al., 2015), the majority of lakes in the CM, SM, WF, NE, and BM sub-regions show.

A^- to HCO_3^- ratios of 1:1, which generally produces waters with pH below 7.5. These lakes show a HCO_3^- content of less than 400 μeq.L^{-1}. Less numerous are a second group of lakes in BM, WF, NE and CM sub-regions characterized by A^- to HCO_3^- ratios of 1:2, which are found to have pH ranging up to 8.0, including HCO_3^- concentrations up to 1000 μeq.L^{-1}. The third group, very limited in number, shows A^- to HCO_3^- ratios of 1:5 present only in lakes NE 9, NE10 and NE11, WF7 and WF8. These can be considered hardwater lakes, with pH values ranging between 8.0 and 8.5. The HCO_3^- concentrations in the hardwater lakes attain concentrations up to 2000 μeq.L^{-1}. Although a few lakes of the BM group seem to achieve a pH higher than 8.0, the HCO_3^- concentrations only attain concentrations up to 1000 μeq.L^{-1}.

Table 2
Carbon 13-DIC, alkalinity, calcite saturation index and pH in RAMP lakes in 2013.

Site	Lake ID	Lat	Lon	δ^{13}C-DIC (‰ VPDB)	Alkalinity (mg.L^{-1})	SI Calcite	pH Field
				(± 0.08)	**(± 0.1)**		**(± 0.3)**
L25	BM1	57.41	-112.93	-14.82	270.8	-1.1089	7.23
175	BM10	57.31	-112.4	-10.01	770	-0.1992	7.41
199	BM11	57.69	-111.91	-21.74	212.2	-1.8761	6.65
L18	BM2	57.42	-112.69	-5.79	478.4	-0.1281	7.79
L60	BM3	57.65	-112.62	-17.08	373.6	-0.7604	7.24
L47	BM4	57.69	-112.74	-16.37	317.4	-0.8932	7.18
L49	BM5	57.76	-112.58	-18.4	167.8	-2.0641	6.38
L28	BM6	57.85	-112.97	-24.31	58.2	-4.0994	4.38
L29	BM7	58.06	-112.27	-25.13	20	-5.7901	6.72
L46	BM8	57.77	-112.4	-17.79	211	-1.5989	7.08
L23	BM9	57.7	-112.38	-16.91	195.6	-1.4979	7.7
E52	CM1	58.77	-115.44	-13.25	687.8	0.1804	7.41
E59	CM2	59.13	-115.13	-9.62	324.8	-0.7099	6.91
E68	CM3	59.19	-115.46	-16.56	238	-1.3167	7
O2	CM4	59.31	-115.35	-16.1	242	-1.2242	6.68
O1	CM5	59.24	-114.53	-22.49	152.6	-1.8326	6.11
L4	NE1	57.15	-110.85	-20.14	1281	-1.6494	8.03
271	NE10	56.64	-110.2	-3.43	1643.4	0.8787	8.02
Kearl	NE11	57.29	-111.24	-3.5	187	0.1909	6.55
L7	NE2	57.09	-110.75	-17.94	384.8	-1.5614	7.36
L8	NE3	57.05	-110.59	-12.64	210.2	-0.9099	6.96
L39	NE4	57.96	-110.4	-12.99	396	-1.3332	7.32
E15 (268)	NE5	56.89	-110.9	-9.28	146.6	-3.8536	7.57
182	NE6	57.27	-110.9	-9.08	867	0.1469	5.37
185	NE7	57.15	-110.86	-24.6	88	-3.4575	7.96
209	NE8	57.23	-110.75	-19.36	258.8	-1.5325	7.67
270	NE9	56.77	-110.91	-3.09	1113.4	0.678	7.37
L107	S1	59.72	-110.02	-4.29	505.6	-0.154	7.39
L109	S2	59.12	-110.83	-12.12	452.4	-0.55	7.6
R1	S3	59.19	-110.68	-10.21	375.4	-0.7127	7.41
A301	S4	59.17	-110.57	-9.65	504.6	-0.3122	7.34
O10	S5	59.13	-110.69	-15.28	257.6	-0.9563	5.01
354	SM1	55.76	-110.76	-8.8	311.4	-0.8774	6.66
A21	SM10	56.26	-111.26	-24.35	42.6	-4.5166	6.72
342	SM2	55.79	-111.83	-16.3	212	-2.0123	5.62
289	SM3	56.2	-111.37	-19.14	120.8	-2.2035	5.73
290	SM4	56.15	-111.23	-25.45	71	-3.6131	5.32
A29	SM5	56.17	-111.55	-24.38	64.2	-3.886	6.78
A26	SM6	56.22	-111.17	-24.66	50.4	-4.2376	6.66
A86	SM7	55.68	-111.83	-18.28	170.6	-1.9185	5.09
287	SM8	56.21	-111.2	-24.5	20	-4.9652	4.76
A24	SM9	56.22	-111.25	-26.13	22.6	-5.0993	7.2
A42	WF1	56.35	-113.18	-12.92	300.8	-0.8858	6.81
A47	WF2	56.24	-113.14	-19.31	229.8	-1.5049	5
A59	WF3	55.91	-112.86	-26.11	54.4	-4.1038	7.24
223	WF4	57.15	-111.98	-13.27	665.8	-0.2673	7.33
225	WF5	56.8	-111.92	-5.77	557.4	-0.3233	6.95
226	WF6	56.81	-111.72	-15.4	399.4	-0.9625	7.61
227	WF7	56.78	-111.79	-9.37	820.8	0.2196	5.12
267	WF8	56.77	-111.95	-5.66	673.8	-0.024	7.59

Finally, a fourth group is represented by S lakes from the Canadian Shield region (Figs. 5 and 7) having A^- to HCO_3^- ratios that follow an unclear non-incremental trend. pH values in this group are less than 8.0 and the HCO_3^- content is lower than 600 μeq.L^{-1}.

As observed in Fig. 7 and described above, most lakes sub-groups are characterized by pH increasing continuously with respect to the total carbonate alkalinity which indicates that in highly dilute lakes, the pH increases are driven by the dissolution of carbonates that are interacting with the CO_2. That interaction promotes the increase in HCO_3^-. Also, ionized carboxylic acid (A-) sourced from dissolved organic matter contributes to the increased alkalinity, but in lower proportion.

3.6. Sources of dissolved carbonate mineral and mineral equilibrium

Sediment core studies in the region were conducted by Hazewinkel et al. (2008), Curtis et al. (2010), Kurek et al. (2013) and Laird et al. (2013) to evaluate acidifications effects mainly through diatom-inferred pH changes in boreal lakes to NE of Alberta and one study to the NE of Saskatchewan. These investigations showed no evidence of widespread lake acidification trends associated with oil sands development (Hazewinkel et al., 2008; Curtis et al., 2010; Mushet et al., 2017; Cook et al., 2017).

Lake sediment cores (Fisher et al., 2009) within the 200-km radius of the AOSR show recurrent stratigraphy comprising organic material and peat at the top, with centimeter-scale alternation of gyttja, glacial sands, silts and organic clays, as well as marls up to 600 mm in thickness. Marl deposits predominate in areas comprising outwash sands and gravels and are primarily generated by moraine deposits (Fisher et al., 2009) typical of the AOSR. Gibson et al. (2019a,b) postulated that carbonate dissolution in surface water was likely enhanced in surface water runoff by the permafrost thaw effect.

We evaluated carbonate mineral saturation states in the RAMP lakes with the program PHREEQC (Table 2). The calcite saturation index (SI), illustrated in Fig. 8 (left panel) is driven by the alkalinity production reaching calcite saturation in lakes NE9, NE10, NE11, WF4, WF5, WF7, WF8, BM2, BM10, CM1, and S4, which were also found to be close to saturation with respect aragonite and dolomite. For the same lakes, enriched $\boldsymbol{\delta^{13}}$ $\mathbf{C_{DIC}}$ values, reaching as high as − 3.4‰ (VPDB), are considered to be indicative of carbonate dissolution. While there is lithological evidence of occurrence of carbonates (marls) in lakes cores (Fisher et al., 2009) that supports the hypothesis of calcite dissolution, there is no direct geochemical evidence from the RAMP watersheds to support the hypothesis of terrestrial or authigenic sources of carbonates, or that these are year-round processes. However, detailed wetland terrain mapping of the RAMP lake watersheds does provide evidence of widespread bog and fen collapse features, particularly in watersheds of the NE, BM and CM sub-regions, although sampling of watershed runoff and permafrost has been limited to isotope sampling at a few sites (Gibson et al., 2015). The relationship between high water yields and permafrost thaw features in RAMP watersheds has been firmly established (Gibson et al., 2019a) and differences between tritium content in RAMP lakes suggests different water sources are flowing to thaw lakes (Gibson et al., 2016). While conducted outside RAMP watersheds, a recent inventory of various non-permafrost wetland types in the region.

including bogs, poor fens, and rich fens established high potential for storage of DIC, DOC and nutrients, especially NH_4^+ in thick, low-permeability peat deposits which extend to 11 m depth in some areas (Gibson et al., 2021). Mobilization of such stores by bog or fen collapse may be an important part of the pH story, although further watershed-based studies will likely be required to confirm this. From arctic regions with degrading permafrost, there is mounting evidence that biogeochemical processing of thawed permafrost substrates will amplify DIC production in lakes (Zolkos and Tank, 2020). We suspect that similar processes are likely occurring in the RAMP lakes, located within a region near the southern limit of permafrost which has been classified as being vulnerable to water resources impacts related to permafrost thaw (Spence et al., 2020).

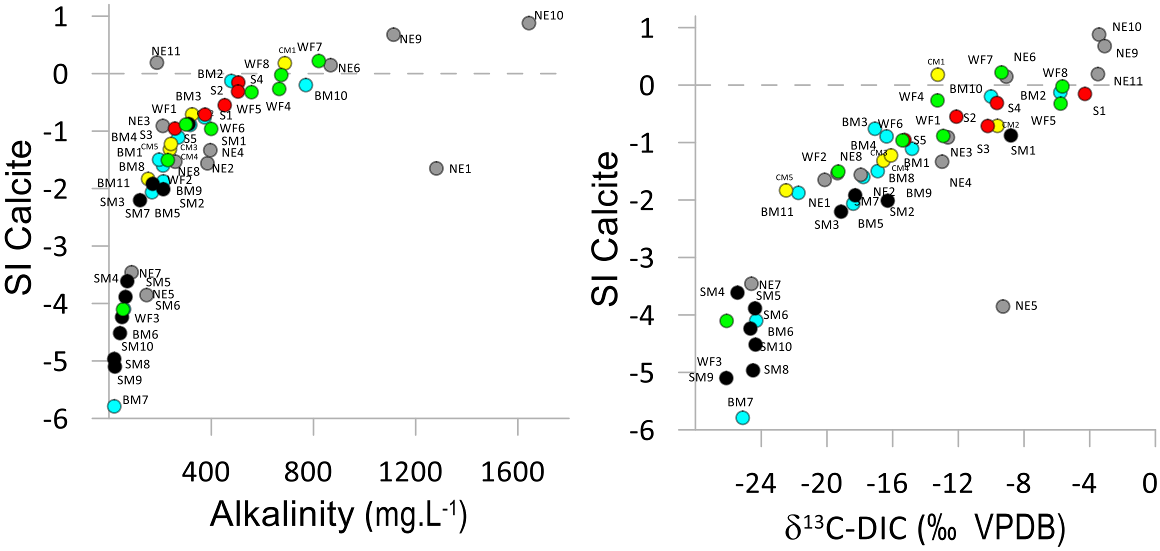

Fig. 8. Calcite saturation in relation to alkalinity or TCA (left) and in relation to $\delta^{13}C_{DIC}$ under lakes summer conditions (June to October 2013).

The softwater lakes are distributed regionally with higher dissolved organic matter and lower alkalinity content seem to show more depleted $\delta^{13}C_{DIC}$ values, in some cases approaching – 24‰ (VPDB) (Fig. 8, Table 2). Noted differences in mineral equilibria between lakes may be substantially explained by differences in the relationship between local geochemical and hydrologic inputs, whereby lakes fed predominantly by shallow flowpaths through peat tend to be more dilute and show alkalinity dominated by organic acids, whereas lakes fed predominantly by groundwater, or lakes containing marl deposits tend to be carbonate buffered. While such processes likely contribute to the observed pH shifts, the permafrost thaw process and its linkage to CO_2 regulation is inferred but cannot be confirmed from data available from this study. We note that input of dissolved carbonate material increases concentrations of HCO_3^- and CO_3^{-2} whereas input of dissolved organic matter increases the ionized carboxylic acids. Given the pH of the lakes, physico-chemical controls established from PCA relationships, and variation in saturation indices, the most important component to understand pH changes is HCO_3^-, and in addition for low pH lakes, the ionized carboxylic acids, which serve to neutralize the hydroxides and hydrogen ions entering the lakes.

Although increases in pH values have been observed in most lakes, Fig. 7 shows that in the AOSR the presence of hardwater lakes with pH values higher than 8.0 (Finlay et al., 2015) is limited to a few (NE9, NE10, NE11, BM10, WF7, WF8).

These lakes show atmospheric pCO_2 in equilibrium with alkalinity (Fig. 8), enriched $\delta^{13}C_{DIC}$ values and may possibly be precipitating authigenic carbonates. These parameters support the hypothesis that the hardwater lakes are fed by groundwater discharge, whereas the softwater lakes with low pH values, supersaturated atmospheric pCO_2 values, low alkalinity concentrations and more depleted $\delta^{13}C_{DIC}$ values (Fig. 8) are characteristic of regional recharge conditions and are likely reliant mainly on surface water. All year monitoring will be required, at least in selected RAMP lakes, to test this hypothesis and to firmly establish the importance of CO_2 evasion on the pH increase.

4. Conclusions

The present study analyzed 15 years of physico-chemical and ion data for 50 RAMP lakes, which are mostly highly-dilute waters. Charge balances were improved and made useful for analysis by incorporating both ionized and total carboxylic acid contents of the waters, and by using these estimates to predict the effect of organic matter dissolution on the alkalinity. PCA analysis, land cover assessments, indirect lithological evidence, apparent pCO_2 estimates, mineral equilibria and $\delta^{13}C_{DIC}$ measurements have provided new insights into the significant role of carbonate dissolution and organic matter dissolution on geochemistry and pH regulation in the lakes. Modeled CO_2 concentrations for the lakes commonly exceeded atmospheric CO_2 estimates, suggesting that lakes at low pH were CO_2 emitters, whereas for lakes with pH greater than 8.5, the CO_2 is transformed into HCO_3^- and CO_3. For these lakes, pCO_2 declines below atmospheric values and we predict leads to hardwater sequestration of atmospheric CO_2 (Finlay et al., 2015). It was apparent that all lakes in the region appeared to be trending towards atmospheric equilibrium at the time of sampling, although seasonality of this process remains to be characterized.

The carboxylic acid contents and organic matter, reflected in the high natural water color, are relatively important to the total alkalinity budget in the watersheds, particularly when the pH values are lower than 7.0. Although the incremental concentrations of bicarbonates and carboxylic acids are present in most lakes, only few lakes show an A^- to HCO_3^- ratio of 1:5 with pH between 8.0 and 8.5 and HCO_3^- concentrations approaching 2000 μeq.L^{-1}. These lakes seem to be in equilibrium with calcite, aragonite and dolomite, and display the most enriched values in $\delta^{13}C_{DIC}$ (between −3.0‰ and −3.5‰ VPDB). These lakes also tend to be dominated by carbonate sources. Low pH, low alkalinity lakes were found to be DOC-rich, were dominated by organic matter dissolution processes, and showed low $\delta^{13}C_{DIC}$ (between −24.0‰ and −18.0‰ VPDB). These results support the assertion that carbonate dissolution as the main mechanism controlling the pH increase in the lakes. In the context of long-term acidification potential, this should be viewed conservatively as a mechanism that may serve to temporarily pause the acidification process, in a similar way to permafrost thaw. Despite the fact that the role of atmospheric CO_2 in the dissolution of carbonates in the watershed headwaters remains pending for further investigation, the resumption of acidification is not certain in the short term. The majority of the RAMP lakes in the boreal Alberta region are considered small therefore the decreasing permafrost melting process has significantly more impact on the net CO_2 relative saturation budget making more difficult to attain rapid theoretical equilibrium than in large alkaline lakes, as those reported by Finlay et al. (2015), from the central Canadian region. Thus, as lakes eventually equilibrate to modified climatic conditions and as oil sands development proceeds across the region the acidification process may be inevitable in the long term.

While informative, PCA, mineral equilibria, pCO_2, and $\delta^{13}C_{DIC}$ relationships would benefit from year-round observations and sampling, at least for selected lakes spanning the overall range of geochemical variability noted across the region in this study. There is also a need to extend hydrologic and geochemical observations to characterize watershed sources, especially via surface runoff sampling and installation and sampling wells in representative terrain units, including collapse scars formed due to permafrost thawing. Such field-based investigations are recommended to improve understanding of the role of allochthonous sources including shallow groundwater within peat, within mineral soils, and bedrock formation waters, if applicable. More field-based information to assess ice-cover duration and its role in modulating carbonate dissolution, CO_2 evasion, pH control would also serve to better understand the observed changes and sustainability of the current trajectory of water quality and quantity changes in the lakes, and how they are expected to affect the regional land mosaic and regional hydrology in general. Surface lake sediments collection would be one strategy to assess the decomposition of organic matter and its effects on calcite saturation in the lakes. Finally, a basic review of current parameters monitored within the water chemistry program is warranted if we now acknowledge that acidifying emissions may not be the only factor impacting the lake chemistry and ecosystem health.

Declaration of Competing Interest

The authors declare that they have no known competing financial interests or personal relationships that could have appeared to influence the work reported in this paper.

Acknowledgments

We thank Colin Cooke, Rob Hazewinkel, and Preston McEachern for ongoing support for incorporation of water sampling for isotopes within the RAMP program over the past 2 decades. Paul Eby, InnoTech Alberta and staff of the Environmental Isotope Laboratory. Funding for the geochemical assessment was obtained from InnoTech Alberta.

References

Aherne, J., Posch, M., 2013. Impacts of nitrogen and sulphur deposition on forest ecosystem services in Canada. Curr. Opin. Environ. Sustain. 5 (1), 108–115. https://doi.org/10.1016/j.cosust.2013.02.005.

Bennett, K.E., Gibson, J.J., McEachern, P.M., 2008. Water yield estimates for critical loadings assessment: comparisons of gauging methods versus and isotopic approach. Can. J. Fish. Aquat. Sci. 65, 83–99.

Birks, S.J., Moncur, M.C., Gibson, J.J., Yi, Y., Fennell, W.J., Taylor, E.B., 2018. Origin and hydrogeological setting of saline groundwater discharges to the Athabasca River: geochemical and isotopic characterization of the hyporheic zone. Appl. Geochem. 98, 172–190. https://doi.org/10.1016/j.apgeochem.2018.09.005.

Birks, S.J., Fennell, J.W., Gibson, J.J., Yi, Y., Moncur, M.C., Brewster, M., 2019. Using regional datasets of groundwater isotope geochemistry to evaluate conceptual models of groundwater flow in the Athabasca Region. Appl. Geochem. 101, 140–159. https://doi.org/10.1016/j.apgeochem.2018.12.013.

Bisogni, J., Arroyo, S., 1991. The effect of carbon dioxide equilibrium on pH in dilute lakes. Water Res. 25 (2), 185–190.

Brook, J.R., Cober, S.G., Freemark, M., Harner, T., Li, S.M., Liggio, J., Makar, P., Pauli, B., 2019. Advances in science and applications of air pollution monitoring: a case study on oil sands monitoring targeting ecosystem protection. J. Air Waste Manag. Assoc. 69 (6), 661–709. https://doi.org/10.1080/10962247.2019.1607689.

Clayer, F., Moritz, A., Gelinas, Yves, Tessier, A., Gobeil, C., 2018. Modeling the carbon isotope signatures of methane and dissolved inorganic carbon to unravel mineralization pathways in boreal lake sediments. Geochim. Cosmochim. Acta 229, 36–52.

Cole, J.J., Caraco, N.F., 1998. Atmospheric exchange of carbon dioxide in a low-wind oligotrophic lake measured by the addition of SF6. Limnol. Oceanogr. 43, 647–656.

Cole, J.J., Prairie, Y.T., 2009. Dissolved CO_2. In: Likens, Gene E. (Ed.), Encyclopedia of Inland Waters, vol. 2. Elsevier, Oxford, pp. 30–34.

Cook, C.A., Kirk, J.L., Muir, D.C., Wiklund, J.A., Wang, X., Gleason, A., Evans, M., 2017. Spatial and temporal patterns in trace element deposition to lakes in the Athabasca oil sands region (Alberta, Canada). Environ. Res. Lett. 12, 1240001. https:doi.org/10.1088/1748-9326/aa9505.

Curtis, C.J., Flower, R., Rose, N., Shilland, J., Simpson, G.L., Turner, S., Yang, H., Pla, S., 2010. Palaeolimnological assessment of lake acidification and environmental change in the Athabasca Oil Sands Region, Alberta. J. Limnol. 69, 92–104.

Devito, K., Creed, I.Gan, Mendoza, T., Petrone, C., Silins U, R., Smerdon, B., 2005. A framework for broad-scale classification of hydrologic response units on the boreal plain: is topography the last thing to consider? – Invited review. Hydrol. Process. 19, 1705–1714.

Eilers, M., Glass, K.E., Webster, A., Arbgalla, A., 1983. Hydrologic control of lake susceptibility to acidification. Can. J. Fish. Aquat. Sci. 4, 1896–1904.

Environment Canada, 2005. Canadian Acid Deposition Science Assessment. Environment Canada, Ottawa, Canada, p. 440.

Finlay, K., Vogt, R., Bogard, M., Wissel, B., Tutolo, B., Simpson, G., Leavitt, P., 2015. Decrease in CO_2 efflux from northern hardwater lakes with increasing atmospheric warming. Nature 519, 215–228.

Fisher, T., Waterson, N., Lowell, T., Hadjas, I., 2009. Deglaciation ages and meltwater routing in the Fort McMurray region, northeastern Alberta and northwestern Saskatchewan, Canada. Quat. Sci. Rev. 28 (2009), 1608–1624.

Gibson, J.J., 2019. Permafrost Thaw as a Mechanism for Widespread pH Increase in Boreal Lakes: Isotopic and Geochemical Evidence. In: Proceedings of the AGU Fall Meeting, 9–13 Dec. 2019, San Francisco.

Gibson, J.J., Edwards, T.W.D., 2002a. Regional surface water balance and evaporationtranspiration partitioning from a stable isotope survey of lakes in northern Canada. Glob. Biogeochem. Cycles 16 (2), 10-1–10-14. https://doi.org/10.1029/2001GB001839.

Gibson, J.J., Prepas, E.E., McEachern, P., 2002b. Quantitative comparison of lake throughflow, residency, and catchment runoff using stable isotopes: modelling and results from a survey of boreal lakes. J. Hydrol. 262, 128–144. https://doi.org/10.1016/S0022-1694(02)00022-7.

Gibson, J.J., Birks, S.J., McEachern, P., Hazewinkel, R., Kumar, S., 2010a. Interannual variations in water yield to lakes in northeastern Alberta: Implications for estimating critical loads of acidity. J. Limnol. 69 (Suppl. 1), 126–134. https://doi.org/10.4081/jlimnol.2010.s1.126.

Gibson, J.J., Birks, S.J., Jeffries, D.S., Kumar, S., Scott, K.A., Aherne, J., Shaw, P., 2010b. Site-specific estimates of water yield applied in regional acid sensitivity surveys in western Canada. J. Limnol. 69 (Suppl. 1), 67–76. https://doi.org/10.4081/jlimnol.2010.s1.67.

Gibson, J.J., Fennell, J., Birks, S.J., Yi, Y., Moncur, M., Hansen, B., Jasechko, S., 2013. Evidence of discharging saline formation water to the Athabasca River in the northern Athabasca oil sands region. Can. J. Earth Sci. 50 (1244–1257), 2013. https://doi.org/10.1139/cjes-2013-0027.

Gibson, J.J., Birks, S.J., Yi, Y., Vitt, D., 2015. Runoff to boreal lakes linked to land cover, watershed morphology and permafrost melt: a 9-year isotope mass balance assessment. Hydrol. Process. 29, 3848–3861. https://doi.org/10.1002/hyp.10502.

Gibson, J.J., Birks, S.J., Yi, Y., 2016. Higher tritium concentrations measured in permafrost thaw lakes, northern Alberta. Hydrol. Process. 30, 245–249. https://doi.org/10.1002/hyp.10599.

Gibson, J.J., Yi, Y., Birks, S.J., 2019a. Isotopic tracing of hydrologic drivers including permafrost thaw status for lakes across northeastern Alberta, Canada: a 16-year, 50-lake perspective. J. Hydrol. Reg. Stud. 26, 100643. https://doi.org/10.1016/j.ejrh.2019.100643.

Gibson, J.J., Birks, S.J., Moncur, M.C., 2019b. Mapping water yield distribution across the southern Athabasca Oil Sands area: baseline surveys applying isotope mass balance of lakes. J. Hydrol. Reg. Stud. 21, 1–13. https://doi.org/10.1016/j.ejrh.2018.11.001.

Gibson, J.J., Yi, Y., Birks, S.J., 2020. Watershed, climate, and stable isotope data (oxygen-18 and deuterium) for 50 boreal lakes in the oil sands region, northeastern Alberta, Canada, 2002-2017. Data Brief 29, 105308. https://doi.org/10.1016/j.dib.2020.105308.

Gibson, J.J., Birks, S.J., Yi, Y., Moncur, M.C., Vallarino, A., Kusel, C., Cherry, M., 2021. Hydrology and geochemistry studies in the oil sands region to investigate the role of terrain conductivity in nitrogen critical loads. Water 2021 (13), 2204. https://doi.org/10.3390/w13162204.

Hanson, P.C., Hamilton, D.P., Stanley, E.H., Preston, N., Langman, O.C., 2011. Fate of allochthonous dissolved organic carbon in lakes: a quantitative approach. PLOS One 6 (7), e21884. https://doi.org/10.1371/journal.pone.0021884.

Hazewinkel, R.O., Wolfe, A.P., Curtis, C.J., Hadley, K., 2008. Have atmospheric emissions from the Athabasca oil sands impacted lakes in northeastern Alberta, Canada? Can. J. Fish. Aquat. Sci. 65, 1554–1567.

Henriksen, A., Kamari, J., Posch, M., Wilander, A., 1992. Critical loads of acidity: nordic surface waters. Ambio 21, 356–363.

Herzeg, A., Hesslein, R., 1984. Determination of hydrogen ion concentration in softwater lakes using carbon dioxide equilibrium. Geochem. Cosmochem. Acta Vol 48, 837–845.

Houle, D., Couture, S., Gagnon, C., 2010. Relative role of decreasing precipitation sulfate and climate on recent lake recovery. Glob. Biogeochem. Cycles 24, 1–11. https://doi.org/10.1029/2009GB003757.

Jasechko, S., Gibson, J.J., Birks, S.J., Yi, Y., 2012. Quantifying saline groundwater seepage to surface water in the Athabasca oil sands region. Appl. Geochem. 10 (10), 2068–2076.

Jeffries, D.S., Semkin, R.G., Gibson, J.J., Wong, I., 2010. Recently surveyed lakes in northern Manitoba and Saskatchewan, Canada: characteristics and critical loads of acidity. J. Limnol. 69 (Suppl. 1), 45–55. https://doi.org/10.4081/jlimnol.2010.s1.45.

Jin, L., Siegel, D.I., Lautz, L.K., Mitchell, M.J., Dahms, D.E., Mayer, B., 2010. Calcite precipitation driven by the common ion effect during groundwater-surface-water mixing: a potentially common process in streams with geologic settings containing gypsum. Bull. Geol. Soc. Am. 122 (7–8), 1027–1038. https://doi.org/10.1130/B30011.1.

Jung, K., Chang, S.X., 2012. Four years of simulated N and S depositions did not cause N saturation in a mixedwood boreal forest ecosystem in the Oil Sands Region in Northern Alberta, Canada. For. Ecol. Manag. 280, 62–70. https://doi.org/10.1016/j.foreco.2012.06.002.

Kling, G.W., Kipphut, G.W., Miller, M.C., 1992. The flux of CO_2 and CH_4 from lakes and rivers in arctic Alaska. Hydrobiologia 240, 23–36.

Korsman, Segerstrom, 1998. Forest fire and lake-water acidity in a northern Swedish boreal area: holocene changes in lake-water quality at Makkassjon. J. Ecol. 86, 112–124.

Krinner, G., 2003. Impact of lakes and wetlands on boreal climate. J. Geophys. Res. Atmos. 108 (D16), 4520.

Kurek, J., Kirk, J.L., Muir, D.C.G., Wang, X., Evans, M.S., Smol, J.P., 2013. Legacy of a half century of Athabasca oil sands development recorded by lake ecosystems. Proc. Natl. Acad. Sci. USA 110, 1761–1766.

Laird, K.R., Das, B., Kingsbury, M., Moos, M.T., Pla-Rabes, S., Ahad, J.M.E., Wiltse, B., Cumming, B.F., 2013. Paleolimnological assessment of limnological change in 10 lakes from northwest Saskatchewan downwind of the Athabasca oils sands based on analysis of siliceous algae and trace metals in sediment cores. Hydrobiologia 720, 55–73.

Lajewski, C.K., Mullins, H.T., Patterson, W.P., Callinan, C.W., 2003. Historic calcite record from the Finger Lakes, New York: impact of acid rain on a buffered terrane. Bull. Geol. Soc. Am. 115, 373–384.

Liggio, J., Li, S.-M., Hayden, K., Taha, Y.M., Stroud, C., Darlington, A., Drollette, B.D., Gordon, M., Lee, P., Leithead A, P., Moussa, S.G., Wang, D., O'Brien, J., Mittermeier, R.L., Brook, J.R., Lu, G., Staebler, R.M., Han, Y., Tokarek, T.W., Osthoff, H.D., Makar, P.A., Zhang, J., Plata, D.L., Gentner, D.R.Liu, 2016. Oil sands operations as a large source of secondary organic aerosols. Nature 534 (7605), 91–94. https://doi.org/10.1038/nature17646.

Liggio, J., StroudJ, C., Wentzell, J.B., Zhang, J., Sommers, J., Darlington, A., Liu, P., Moussa, S.G., Leithead, A., Hayden K, K., 2017. Quantifying the primary emissions and photochemical formation of isocyanic acid (HNCO) downwind of oil sands operations. Environ. Sci. Technol. 51 (24), 14462–14471. https://doi.org/10.1021/acs.est.7b04346.

Liggio, J., Le, S., Staebler, R., Hayden, K., Darlington, A., Mittemeier, R., O'Brien, J., McLaren, R., Wolde, M., Worthy, D., Vogel, F., 2019. Measured Canadian oil sands CO_2 emissions are higher than estimates made using internationally recommended methods. Nat. Commun. 10, 1863 https://doi.org/10.1038/s41467-019-09714-9.

Makar, P.A., Akingunola, A., Cole, A.S., Aklilu, Y., Zhang, J., Wong, I., Hayden, K., Li, S., Kirk, J., Scott, K., Moran, M.D., Robichaud, A., Cathcart, H., Baratzedah, P., Pabla, B., Cheung, P., Zheng, Q., Jefffries, D.S., 2018. Estimates of exceedances of critical loads for acidifying deposition in Alberta and Saskatchewan. Atmos. Chem. Phys. 18, 9897–9927.

Mattson, M.D., Likens, G.E., 1992. Redox reactions of organic matter decomposition in a soft water lake. Biogeochemistry 3, 149–172.

Mushet, G.R., Laird, K.R., Das, B., Hesjedal, B., Leavitt, P.R., Scott, K.A., Simpson, G.L., Wissel, B., Wolfe, J.D., Cumming, B.F., 2017. Regional climate changes drive increased scaled-chrysophyte abundance in lakes downwind of Athabasca Oil Sands nitrogen emissions. J. Paleolimnol. 58 (3), 419–435. https://doi.org/10.1007/s10933-017-9987-6.

Oliver, B., Thurman, E., Malcolm, R., 1983. The contribution of humic substances to the acidity of colored natural waters. Geochem. Cosmochem. Acta 47, 2031–2035.

Parkhurst D.L. and Appelo C.A.J. 1999. Description of Input and Examples for PHREEQC.Version 3.5.0.14000. A Computer Program for Speciation, Batch-Reaction, One-Dimensional Transport, and Inverse Geochemical Calculations.

Prepas, E.E., Planas, D., Gibson, J.J., Vitt, D.H., Prowse, T.D., Dinsmore, W.P., Halsey, L.A., McEachern, P.M., Paquet, S., Scrimgeour, G.J., Tonn, W.M., Paszkowski, C. A., Wolfstein, K., 2001. Landscape variables influencing nutrients and phytoplankton communities in boreal plain lakes of northern Alberta: a comparison of wetland- and upland-dominated catchments. Can. J. Fish. Aquat. Sci. 58, 1286–1299.

Remberg, I., Korsman, T., Birks, H.J.B., 1993. Prehistoric increases in the pH of acid-sensitive Swedish lakes caused by land-use changes. Nature 363, 824–827.

Roberts, K.E., Lamoureux, S.F., Kyser, T.K., Muir, D.C.G., Lafrenière, M.J., Iqaluk, D., Pieńkowski, A.J., Normandeau, A., 2017. Climate and permafrost effects on the chemistry and ecosystems of high arctic lakes. Sci. Rep. 7, 1–8. https://doi.org/10.1038/s41598-017-13658-9.

Schmidt, A., Gibson, J.J., Santos, I.R., Shubert, M., Tattrie, K., Weiss, H., 2010. The contribution of groundwater discharge to the overall water budget of lakes in Alberta/Canada estimated from a radon mass balance. Hydrol. Earth Syst. Sci. 14, 79–89.

Scott, K.A., Wissel, B., Gibson, J.J., Birks, S.J., 2010. Limnological characteristics and acid sensitivity of boreal headwater lakes in northwest Saskatchewan, Canada. J. Limnol. 69 (Suppl. 1), 33–44. https://doi.org/10.4081/jlimnol.2010.s1.33.

Shapley, M.D., Ito, E., Donovan, J.J., 2005. Authigenic calcium carbonate flux in groundwater-controlled lakes: implications for lacustrine paleoclimate records. Geochem. Cosmochem. Acta 69 (No. 10), 2517–2533.

Smerdon, B.D., Devito, K.J., Mendoza, C.A., 2005. Interaction of groundwater and shallow lakes on outwash sediments in the sub-humid Boreal Plains of Canada. J. Hydrol. 314, 246–262.

Spence, C., Norris, M., Bickerton, G., Bonsal, B.R., Brua, R., Culp, J.M., Dibike, Y., Gruber, S., Morse, P.D., Peters, D.L., Shrestha, R., Wolfe, S.A., 2020. The Canadian water resource vulnerability index to permafrost thaw (CWRVIPT). Arct. Sci. 6 (2020), 437–462 dx.doi.org/10.1139/as-2019-0028.

Wan, C., Gibson, J.J., Shen, S., Yi, Y., Yi, P., Yu, Z., 2019. Using stable isotopes paired with tritium analysis to assess thermokarst lake water balances in the Source area of the Yellow River, northeastern Qinghai-Tibet Plateau, China. Sci. Total Environ. 689, 1276–1292. https://doi.org/10.1016/j.scitotenv.2019.06.427.

Wan, C., Gibson, J.J., Peters, D.L., 2020. Isotopic constraints on water balance of tundra lakes and watersheds disturbed by permafrost degradation in the Mackenzie Delta region, Northwest Territories, Canada. Sci. Total Environ. 731, 139176 https://doi.org/10.1016/j.scitotenv.2020.139176.

Whitfield, C., Aherne, J., Gibson, J., Seabert, T., Watmough, S., 2010. The controls on boreal peatland surface water chemistry in Northern Alberta, Canada. Hydrol. Process. 24, 2143–2155.

Wolfe, A.P., 2001. Climate modulates the acidity of Arctic lakes on millennial time scales. Geology 30, 215–218.

Zolkos, S., Tank, S.E., 2020. Experimental evidence that permafrost thaw history and mineral composition shape abiotic carbon cycling in thermokarst-affected stream networks. Front. Earth Sci. 8, 152. https://doi.org/10.3389/feart.2020.00152.